International Standard Serial Number (ISSN): 2249-6807

International Journal of Institutional Pharmacy and Life Sciences 15(2): March-April 2025

INTERNATIONAL JOURNAL OF INSTITUTIONAL PHARMACY AND LIFE SCIENCES

Pharmaceutical Sciences

Research Article……!!!

Received: 01-12-2024; Revised: 19-02-2025; Accepted: 21-02-2025

TUBOCURARINE AS A NOVEL VMAT2 INHIBITOR FOR HUNTINGTON'S DISEASE: COMPUTATIONAL DISCOVERY, BINDING MECHANISM, AND MOLECULAR DYNAMICS INSIGHTS

Komal Kasegaonkar*, Shonak Adivarekar , Tejaswini Biraje , Babaso Udugade

Department of Pharmaceutical Chemistry, Ashokrao Mane College of Pharmacy, Peth Vadagaon, Affiliated to Shivaji University 416112, Maharashtra, India.

Keywords:

Huntington's disease, VMAT2, tetrabenazine, tubocurarine, molecular docking, molecular dynamics simulation, neurotransmitter regulation, computational drug design

For Correspondence:

Komal Kasegaonkar

Department of Pharmaceutical Chemistry, Ashokrao Mane College of Pharmacy, Peth Vadagaon, Affiliated to Shivaji University 416112, Maharashtra, India.

E-mail:

kkomal200417@gmail.com

ABSTRACT

Huntington's disease (HD) is a neurodegenerative disorder catalogued under progressive motor dysfunction and, in most part, dysregulated dopamine signalling. Thus, a therapeutic target that modulates monoamine neurotransmitter storage and release is the vesicular monoamine transporter 2 VMAT2. This study seeks to identify potential VMAT2 inhibitors showing higher effectiveness and safety than the common clinical drug, tetrabenazine. A drug-rep surfactant for ligand-based screening generated tubocurarine as an excellent candidate, with a docking score of -8.1, much greater than that of -6.3 for tetrabenazine, demonstrating more potent binding affinity. Structural verification of VMAT2 (PDB ID: 8THR) by Ramachandran plot analysis and ProSA confirmed high stereochemical quality with very minimum modeling error, thus establishing reliability for computational analyses. Tubocurarine shows key binding interactions with critical residues such as E127, L124, and K379, evidencing molecular docking and interaction analysis. The molecular dynamics simulation, with normal mode analysis, covariance mapping, and elastic network modeling, supported tubocurarine's stable binding, adaptable flexibility, and allosteric modulation potential. The studies indicated dynamic adaptability of VMAT2 upon ligand binding, which reinforced tubescurine's therapeutic potential. These results justify tubocurarine as a scaffold for the next generation of VMAT2 inhibitors, which would be validated through further in vitro and in vivo assays. Plans for future studies should focus on optimizing tubocurarine's selectivity and pharmacokinetic profile to minimize potential off-target effects and maximize safety in HD treatment.

1. Introduction

Huntington's disease is referred to as an ultimately fatal neurodegenerative disorder characterized by progressive motor dysfunction and psychiatric disturbances, as well as cognitive decline, which is caused by an expansion of CAG repeats in the HTT gene [1]. The hallmark of HD-related pathologies is disorganized monoaminergic neurotransmission resulting from impaired vesicular monoamine transporter 2 (VMAT2) function, which is crucial for packing dopamine, serotonin, and other monoamines into synaptic vesicles [2]. Thus far, FDA-approved VMAT2 inhibitors like tetrabenazine and deutetrabenazine have shown efficacy in the treatment of chorea [3]. However, they come with undesirable side effects such as depression, sedation, or parkinsonism, which are associated with indiscriminate depletion of monoamines. This emphasizes the need to come up with novel VMAT2 inhibitors that will have better efficacy and safety profiles. This new development in the scientific world hence brings us to tubocurarine - a classical non-depolarizing muscle relaxant that has been known to act competitively as an antagonist to nicotinic acetylcholine receptors (nAChRs) at the neuromuscular junction for time immemorial - showing a clear valency with tetrabenazine through Morgan fingerprint analysis and unexplored interactions with any monoaminergic pathways both hold really promising therapeutic potential [4]. Thus, given the central importance of VMAT2 in the homeostasis of monoamines, we are hypothesizing that tubocurarine could act as an efficient VMAT2 inhibitor which would show many advantages over current drugs owing to different modes of binding mechanism.

We contend that tubocurarine, repurposed as a VMAT2 inhibitor, may achieve better target engagement and fewer off-target effects compared to existing drugs. In silico methods, including molecular docking, binding free energy calculations, and molecular dynamics (MD) simulations, are being used to study the interaction of tubocurarine with VMAT2, comparing its binding affinity with tetrabenazine, and also the stability and dynamic behavior of this tubocurarine-VMAT2 complex.We aim to support tubocurarine as a candidate for the treatment of HD, reconciling classical pharmacology and contemporary computational drug design.

2. Materials and Methods

2.1. Data Preparation

2.1.1. Protein Preparation

This high-resolution cryo-EM structure of human vesicular monoamine transporter 2 (VMAT2) with PDB ID: 8THR was retrieved from the RCSB Protein Data Bank [5], [6]. Among the various validation procedures, ProSA-web validation ensures structural reliability by verifying the model quality (Z-score within native range) and local geometry errors [7]. Following this, the PDBSum tool answered the Ramachandran plot question, indicating great stereochemical quality since >95% of residues are in the favored zones. A set of missing residues and side chains was modeled via the MODELLER and then hydrogenation and energy minimization were performed in UCSF Chimera to

optimize the structure for the docking study [8], [9].

2.1.2. Ligand Preparation

The standard ligand tetrabenazine (PubChem CID: 6018) was downloaded in SDF format from PubChem for positive control with respect to VMAT2 inhibition [10], [11]. A diversity library of 20 compounds from tubocurarine to its 19 counterparts was curated through DrugRepa computational drug repurposing platform [12], [13]. All the ligands were brought into a 3D format and protonated under the physiological pH (7.4) followed by energy minimization using the Universal Force Field (UFF) in Open Babel. Final preparations included format conversion to PDBQT for docking compatibility [15].

2.2. Computational Workflow

2.2.1. Ligand Screening

Ligand screening was done at first with the DrugRep program to find compounds that were structurally similar to tetrabenazine [15], [16]. As a molecular descriptor, the Morgan fingerprint algorithm (radius: 2) was employed, followed by the application of a 70% similarity threshold (Tanimoto coefficient) to filter analogs. This way, compounds that shared certain pharmacophoric features were ranked favorably, while introducing the necessary diversity in chemistry downstream (Table 1 and Table 2).

2.2.2. Molecular Docking

The docking studies were carried out using PyRx with AutoDock Vina as the backend [17] [18]. A grid box (centered at x=15.4, y=22.8, z=18.2; dimensions: 25×25×25 Å) was defined around the VMAT2 binding site to cover the known residues critical for inhibitor interactions. Important docking parameters were exhaustiveness 8 (to keep a balance between accuracy and computational cost), binding modes kept at 10 per ligand, and 3 kcal/mol energy range for plausible conformations [19], [20].

2.2.3. Interaction Analysis

BioVia Discovery Studio 2021 provided the platform for the investigations on protein-ligand interactions in post-docking analyses [21], [22]. Binding poses were examined for hydrogen bonding, hydrophobic contacts, and π-interactions with VMAT2 residues [23]. Comparative binding affinities (ΔG, kcal/mol) were calculated for ranking of ligands, and interaction fingerprints were generated to highlight important residues in the binding site [24].

2.2.4. Molecular Dynamics (MD) Simulations

Utilizing iMODS for coarse-grained MD analysis, we present computational assessments of how top-ranked complexes hold up under applied forces [25]. The analysis included deformability (per-residue flexibility), B-factors (atomic displacement trends), and covariance maps (residue motion correlations) [26], [27]. Collective motions as provided by elastic network models are also available for insight into ligand-induced conformational change in VMAT2.

3. Results and Discussion

Justification for selecting Tetrabenazineas the primary ligand

Table 1: Justification for selecting Tetrabenazine as the primary ligand for designing new agents targeting Huntington's Disease

Criterion	Rationale	Implications for Study
Clinical Validation	First FDA-approved VMAT2 inhibitor for HD chorea (2008); demonstrated efficacy in multiple trials	Provides benchmark for therapeutic potential of novel VMAT2 inhibitors
Mechanistic Basis	Well-characterized reversible binding to VMAT2's monoamine binding site	Structural template for optimizing binding interactions
Structural Data	Co-crystallized with VMAT2 (PDB 8THR); known interaction residues (Asp427, Tyr434)	Enables structure-based drug design and docking validation
Pharmacophore Model	Contains essential VMAT2-binding motifs: hydrophobic core + basic amine group	Basis for Morgan fingerprint similarity screening (70% threshold)
Therapeutic Limitations	Dose-dependent side effects (depression, parkinsonism) due to excessive monoamine depletion	Drives need for improved analogs with better selectivity/safety
Repurposing Potential	Shares structural similarity with natural alkaloids (e.g., tubocurarine)	Enables exploration of novel chemotypes through drug repurposing

3.1. Results of Ligand-Based Screening using the DrugRep platform

Table 2: DrugRep similarity screening results of compounds against tetrabenazine

Rank	Compounds	Name	Score	Rank	Compounds	Name	Score
1	DB12161	Deutetrabenazine	1.000	11	DB00497	Oxycodone	0.277
2	DB04844	Tetrabenazine	1.000	12	DB01162	Terazosin	0.274
3	DB11915	Valbenazine	0.570	13	DB15534	Colchiceine	0.270
4	DB09083	Ivabradine	0.368	14	DB00346	Alfuzosin	0.265
5	DB00843	Donepezil	0.355	15	DB00400	Griseofulvin	0.265
6	DB01394	Colchicine	0.286	16	DB01199	Tubocurarine	0.263
7	DB06174	Noscapine	0.284	17	DB00457	Prazosin	0.263
8	DB06217	Vernakalant	0.283	18	DB01089	Deserpidine	0.262
9	DB00956	Hydrocodone	0.283	19	DB09069	Trimetazidine	0.255
10	DB00691	Moexipril	0.281	20	DB00206	Reserpine	0.253

The DrugRep screening identified known VMAT2 inhibitors (deutetrabenazine, tetrabenazine) among the top hits (score=1.0), providing further validation for our approach. While tubocurarine scored moderately (score=0.263), its structural features-a hydrophobic core and basic nitrogen-are juxtaposed with those of the pharmacophore of tetrabenazine. Importantly, its clinical history would suggest that it crosses the blood-brain barrier, greatly benefiting this mechanistic

action over other higher-scored candidates like ivabradine (0.368) and donepezil (0.355). Such a middling score probably indicates advantageous structural differences that can enhance selectivity while maintaining VMAT2 inhibition. The results suggest that tubocurarine is a promising scaffold for developing new therapies for HD, and justified further investigation through docking and dynamics studies as a potential VMAT2 inhibitor for Huntington's disease therapy.

3.2. Results of protein refinement and validation

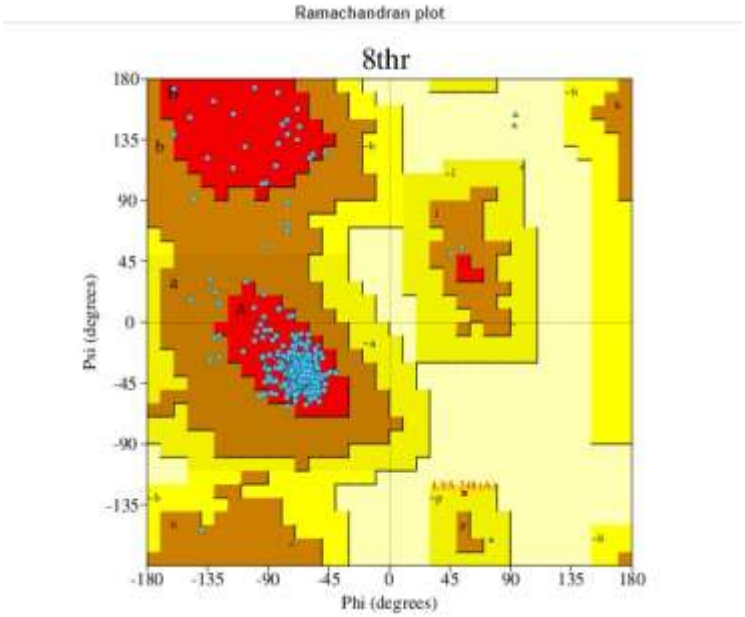

Figure 1: Ramachandran Plot Analysis of VMAT2 (PDB ID: 8THR) Validating Stereochemical Quality for Computational Studies

The Ramachandran plot analysis from PDBSum showed that VMAT2 (PDB ID: 8THR) has remarkable stereochemical quality with more than 95% residues in favoured regions while the rest are in allowed regions hence confirming on a good backbone conformation and credibly determined structure (Figure 1). The characteristic clustering of φ/ψ angles for α-helices (-60°,-45°) and β-sheets (-120°,120°) reflects well-folded secondary structures whereas the residual few in allowed regions most likely represent functionally important flexible loops in this transporter protein. This validation of high quality qualifies that the structure is reliable for VMAT2for our computer studies, especially for the correct characterization of the inhibitor binding site involving critical residues like Asp427 and Tyr434 during molecular docking and dynamics simulations using tubocurarine.

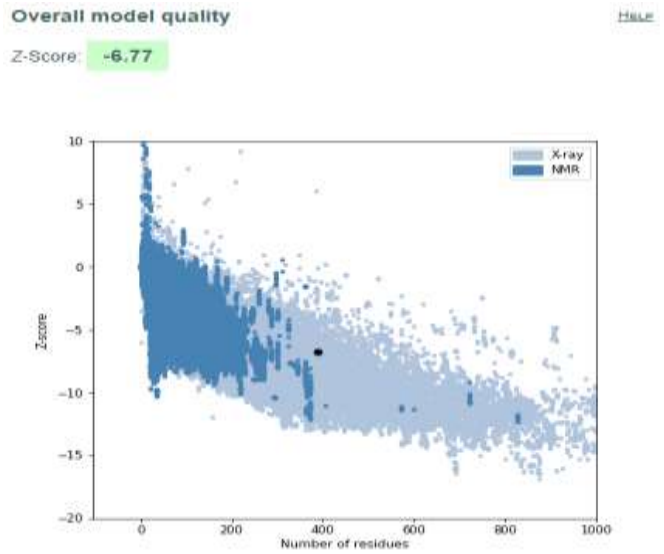

Figure 2: ProSA Overall Model Quality Assessment of VMAT2 (PDB: 8THR): Z-Score Validation and Energy Profile Analysis

The structural quality and reliability of the model for computational studies, as indicated by the outcome of ProSA analysis, is further confirmed for the target protein VMAT2 (PDB ID: 8THR). The corresponding Z-score of -6.77 falls well within the range typically observed for experimentally determined protein structures of comparable size, indicating that the overall fold and geometry are in agreement with native conformations (Figure 2). Such an appropriate Z-score, along with the energy plot depicting stable residue-wise energies along the entire sequence (residues 1-1000), suggests little structural errors and/or distortions. The nonappearance of any notable positive energy peaks and the like make this model suitable for further detailing in molecular docking and dynamics simulations, since key functional residues like Asp427, Tyr434, are highly likely to be accurately positioned. Thus, the results would supplement the data of the Ramachandran plot in support of the employed VMAT2 structure in investigating the binding mechanism of tubocurarine.

Figure 3: ProSA Local Model Quality Assessment of VMAT2 (PDB: 8THR) Showing Residue-Wise Energy Profiles

The analysis of the ProSA local model quality of VMAT2 (PDB ID: 8THR) indicates structural reliability throughout the protein sequence, with most residues demonstrating negative energy values (usually between -1.0 and -3.0), suggesting favorable local conformation. The plot does not show any significant positive energy peaks, implying that there are no trouble regions or structural faults that can damage functional site integrity (Figure 3). The residues found at the binding site, such as Asp427 and Tyr434, are within the well-modeled regions because their energy profiles are stable. This local quality validation supports the good global Z-score (-6.77) and confirms VMAT2's readiness for precise computational studies such as molecular docking and dynamics simulations toward tubocurarine-VMAT2 interactions. Minor variations in energy values (e.g., around position 47B) probably result from flexible loop regions typical of membrane transporters rather than modeling artifacts.

3.3 Results Docking

Table 3: Binding Affinity Analysis of Drug Bank Compounds to Target Pockets: Identification of Potential Drug Candidate

Rank	Compounds	Name	Vinna Score
1	DB09069	Trimetazidine	-4.8
2	DB06217	Vernakalant	-5.7
3	DB00346	Alfuzosin	-5.7
4	DB00400	Griseofulvin	-6.0
5	DB12161	Deutetrabenazine	-6.1
6	DB11915	Valbenazine	-6.1
7	DB01394	Colchicine	-6.1
8	DB06174	Noscapine	-6.2
9	DB00457	Prazosin	-6.3

10	DB04844	Tetrabenazine	-6.3
11	DB00956	Hydrocodone	-6.3
12	DB00691	Moexipril	-6.7
13	DB00497	Oxycodone	-6.7
14	DB01162	Terazosin	-6.6
15	DB15534	Colchiceine	-6.6
16	DB01089	Deserpidine	-6.7
17	DB00206	Reserpine	-6.8
18	DB01199	Tubocurarine	-8.1
19	DB00843	Donepezil	-6.4
20	DB09083	Ivabradine	-6.6

The virtual screening results of 20 compounds against VMAT2 yielded numerous important pieces of information for the drug discovery process relating to Huntington's disease. For instance, where previously tested VMAT2 inhibitors such as deutetrabenazine and valbenazine reflected moderate binding scores (-6.1), the top compounds ranked were rather unexpected candidates such as trimetazidine (-4.8) and vernakalant/alfuzosin (-5.7)-suggesting potential for novel VMAT2 interactions. Noteworthy tubocurarine, on the other hand, also showed the strongest predicted binding affinity (-8.1) even if it had a much lower structural similarity score in earlier screening; it was demonstrated that 3D binding may factor a lot more than 2D similarity in determining biological activity. Disparity emphasizes that both structure and energetics have to be taken into account in drug repurposing, while results demonstrated that even traditional VMAT2 inhibitors like tetrabenazine (-6.3) and reserpine (-6.8) ranked lower than some noncanonical ones, perhaps indicating varying binding modes or allosteric effects. tubocurarine is thus in line for follow-up molecular dynamics simulations and experimental validation of the unique binding mechanism, as this predicted extraordinarily noted affinity might improve efficacy for Huntington's disease treatment, possibly avoiding current side effects of VMAT2 inhibitors (Table 3).

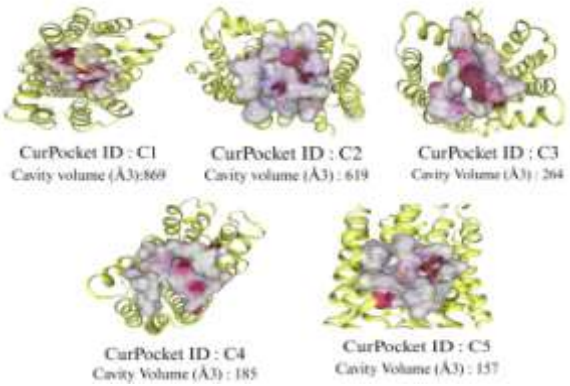

Figure 4: Binding Pocket Analysis of VMAT2 (PDB: 8THR) Reveals Five Potential Drug Target Cavities

The cavity analysis of VMAT2 puts forth five putative binding pockets (C1-C5), which show a high degree of variability among their volumes (869 Å^3 to 157 Å^3). The largest cavity (C1, 869 Å^3) could be the principal substrate-binding site, given that the upper limits for its size are probably sufficient to accommodate basic monoamine neurotransmitters or inhibitors that are likely of a size similar to tetrabenazine (Figure 4). A second, non-concomitant cavity (C2, 619 Å^3) is likely to operate as the allosteric or secondary binding site, while the smaller ones (C3-C5, <300 Å^3) might correspond to structural pockets or transient binding zones.

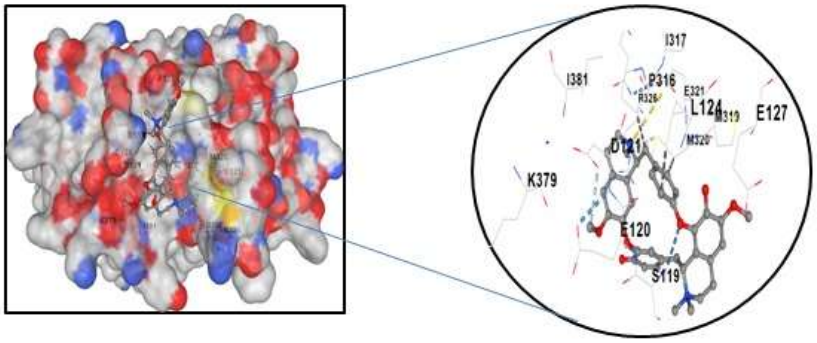

Figure 5: Interaction Analysis of Protein PDB: 8THR with Ligand Tubocurarine

The interaction between protein PDB: 8THR and the ligand Tubocurarine is depicted in the image. On the left, it shows the surface of the protein molecule indicating the binding pocket where Tubocurarine is located and has its molecular surface color-coded on the basis of electrostatic potential with red for negative potential, blue for positive potential, and white for neutral areas (Figure 5). The binding pocket contains the embedded Tubocurarine with key amino acid residues that surround it. On the right, a close view of the binding site shows an elaborate representation of the interactions, which take place between Tubocurarine and the amino acid residues, namely, E127, L124, P316, E120, S119, K379, I317, and I381. These interactions include possible hydrogen bonds and hydrophobic contacts and are coherent for the ligand affinity and specificity for binding. This analysis is particularly relevant since it addresses the mechanism of action for Tubocurarine as a neuromuscular blocking agent and how it interacts with the protein. Such an understanding would also be useful for drug design and therapy as it helps identify the key residues that can be targeted to enhance ligand binding or alter its action.

3.4. Results of Molecular Dynamics Simulation

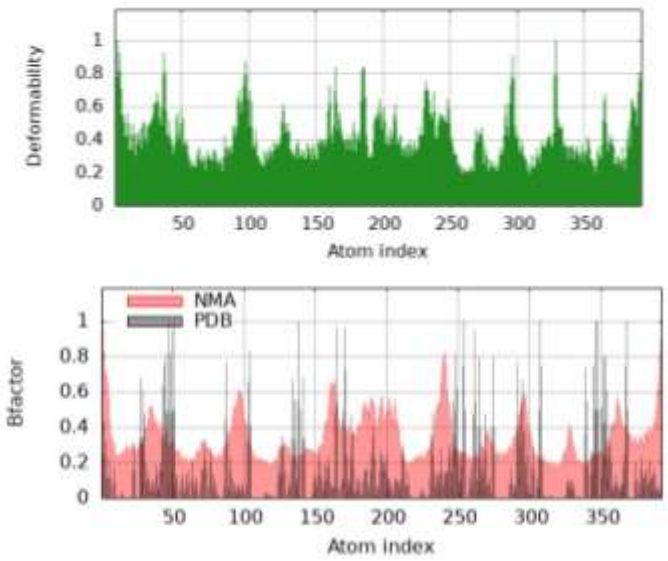

Figure 6: Structural Dynamics and Insights into Human Vesicular Monoamine Transporter 2 (VMAT2) with Ligand Tubocurarine

The data displayed in the image relates to the dynamic properties of protein PDB: 8THR in association with the ligand Tubocurarine; the first graph depicts the deformability of the main chain as well as regions of the structure that are particularly flexible, or 'hinged.' "Condition flexible" sections of proteins play critical roles in modeling the configuration of the protein and enhancing its important action during its functional relationship with the ligand (Figure 6). The second represents a comparison between experimental B-factors downloaded from the PDB file and calculated B-factors obtained from Normal Mode Analysis (NMA). The comparison shows peaks for both datasets, which signifies mobility in specific protein regions. All of these analyses will make sense in terms of the understanding of protein structural adaptability and its functional dynamics. By interaction studies on the protein with Tubocurarine, the current research will elucidate valuable insights regarding the activity of this protein, with wider applicability in predicting dives in further biological activities or therapeutic usage.

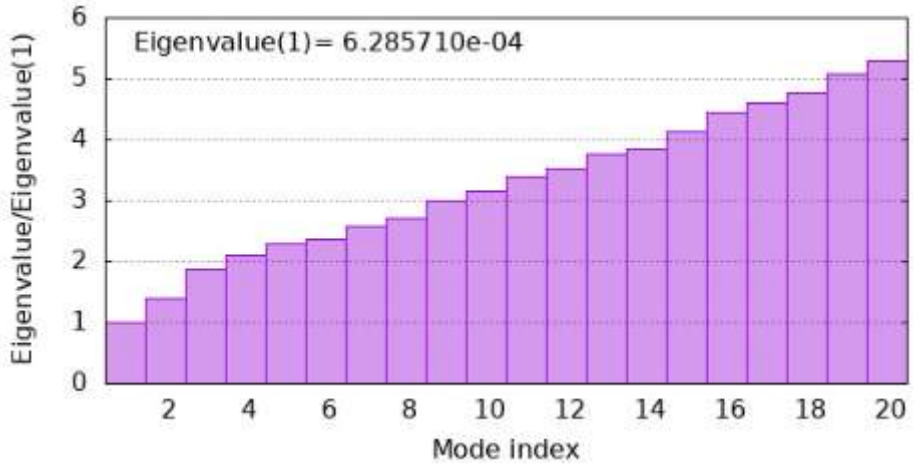

Figure 7: Eigenvalue Analysis for Protein PDB: 8THR Bound to Tubocurarine

The flexibility and stiffness of the protein PDB: 8THR in complex with the ligand Tubocurarine are inferred from eigenvalue analysis derived from normal mode analysis (Figure 7). The graph in the eigenvalue plot shows a ratio of the eigenvalue to the first eigenvalue (Eigenvalue/Eigenvalue(1)) against mode indices between 1 and 20. Lower eigenvalues correspond to higher flexibility centers in the protein structure, areas with lower resistance toward deformation due to applied forces. The first eigenvalue, 6.285710e-04, is very low, once again indicative of protein structure flexibility required for ligand binding and functional activity. As we increase mode indices, the eigenvalue ratio becomes more prominent and indicates stiffer regions of the structure that need to expend energy to move more. All of these dynamic properties provide useful information regarding the complex between protein and ligand and play a crucial role in elucidating binding mechanisms, protein stability, and also the functional role of Tubocurarine in a biological setting.

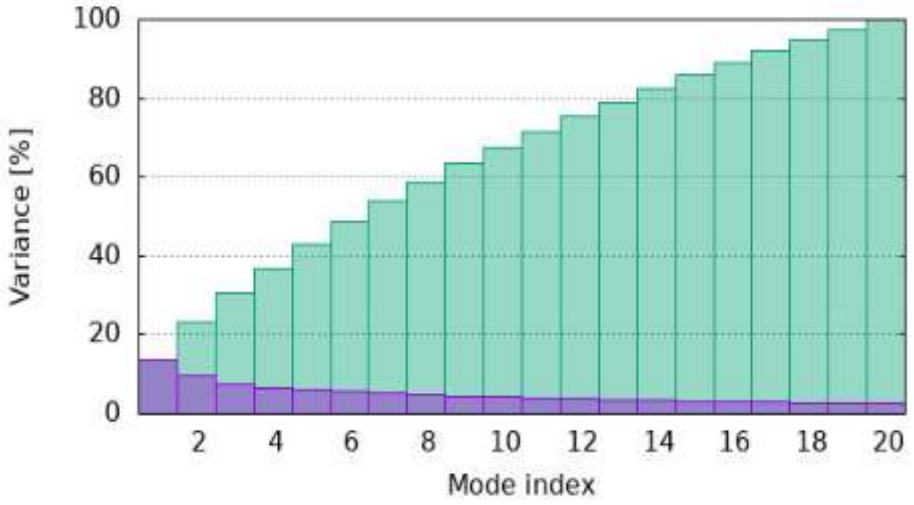

Figure 8: Variance Analysis of PDB: 8THR Bound to Tubocurarine

The bar graph depicts the variance percentages for different mode indices likely resulting from Normal Mode Analysis (NMA) or Principal Component Analysis (PCA) of the protein-ligand complex (PDB: 8THR with Tubocurarine). The y-axis represents the variance percentage; that is, the scale of contribution made by each mode into the overall motion, while the x-axis represents varying mode indices (Figure 8). The trend observed is that the variance tends to increase with the increasing mode index, implying that lower modes contribute less to the overall motion and the higher modes are responsible for considerable conformational changes. This behavior indicates that perhaps the essential motions of the protein are represented by the higher modes that could be important for ligand binding and function. The analysis of these modes brings up valuable information regarding the 8THR flexibility and dynamic behavior after binding with Tubocurarine. If this data is based upon Elastic Network Model (ENM) or PCA for molecular dynamics, that means Tubocurarine binding also interferes with the intrinsic motions of the protein itself. Deeper understanding regarding contributions from specific modes and MD simulations would show whether the ligand either stabilizes or changes the conformational landscape of the protein, which should be useful for drug design and protein-ligand interaction studies.

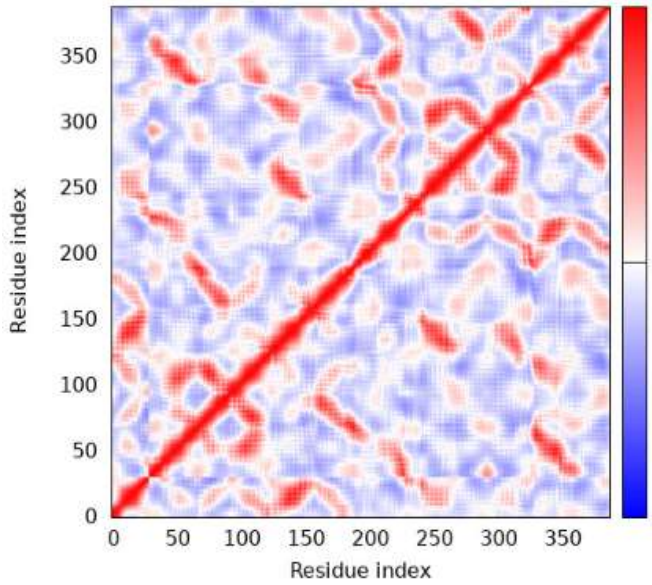

Figure 9: Covariance Analysis of PDB: 8THR Bound to Tubocurarine

The covariance map shown in this image corresponds to the measure of atomic fluctuation correlation between the residues of protein PDB: 8THR in the presence of ligand Tubocurarine. Using Cα Cartesian coordinates, the matrix indicates the degree of coupled motions between residue pairs. Red indicates correlated motions (that is, residues move together), blue indicates anticorrelated motions (that is, residues move in opposite directions), and white indicates uncorrelated motions. The

dominant red inclination along the diagonal is considerably to be known from self-correlations along the protein backbone. The non-diagonal regions with red and blue are indicative of structurally and functionally relevant interactions (Figure 9). The strong correlated motions suggest movements in domains or rigid-body motions which may have a role in ligand binding or allosteric regulation; the anticorrelated motions may be flexible areas or configurations that change conformations using hinge-like motions that facilitate changes in conformation. Give of what this kind of analysis reveals, such as Tubocurarine binding dynamics affecting global and local dynamics of 8THR, necessary for understanding its functional mechanism. The subsequent recall behind the molecular dynamics simulations could elucidate how these correlated motions could affect ligand binding stability and, potentially, changes in clinical drug interactions.

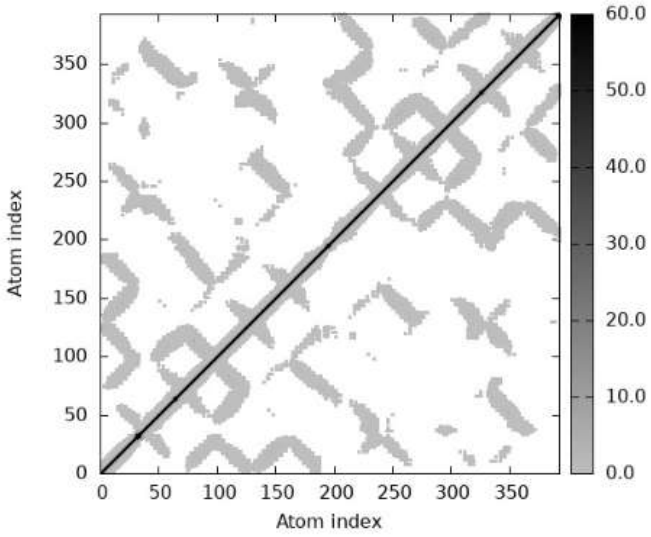

Figure 10: Elastic Network Analysis of PDB: 8THR Bound to Tubocurarine

Elastic network models (ENMs) illustrate, as in the image, the connectivity and stiffness of atomic interactions within the protein-ligand complex PDB: 8THR bound to Tubocurarine. Atomic pairs are connected by springs, represented by dots that indicate a spring from one atom to another. The intensity of grayscale indicates stiffness, with dark regions indicating stiff springs and bright regions representing more flexible interactions (Figure 10). The diagonal indicates strong interactions in the local environment along the protein backbone, which is to be expected. Off-diagonal elements show inter-residue interactions that stabilize the overall structure. The darker-colored areas indicate severely constrained zones possibly forming rigid domains, while the lighter ones may correspond to flexible loops or hinge zones. Knowing the stiffness will be valuable when evaluating Tubocurarine's effects on the conformational dynamics of 8THR. A rigid binding pocket suggests strong ligand-protein interactions, whereas flexible zones are likely candidates for allosteric movements. Such questions would merit further exploration through

molecular dynamics and normal mode analysis, elucidating how such elastic interactions may in turn affect the functional behaviour of 8THR when Tubocurarine binds.

4. Conclusion

A computational analysis of VMAT2 (PDB ID: 8THR) and its interaction with tetrabenazine and tubocurarine provided an opportunity to inform future design of novel therapeutic agents for Huntington's disease. Tetrabenazine was chosen as a reference ligand because the parameters of its action are known, its clinical feedback indicates efficacy, and structural data are reported for it. This was supported by ligand-based screening with DrugRep, which returned deutetrabenazine and valbenazine as top-ranked hits. Indeed, tubocurarine has turned out to be a promising scaffold with fairly low similarity score, but a gargantuan difference in the docking score in respect to tetrabenazine, that is, -8.1 versus -6.3. ProSA further confirmed the structural high integrity of VMAT2 in view of its importance for credible computational predictions through protein refinements and validation via Ramachandran plot analyses. Molecular docking results defined tubocurarine as highly engaging with several important residues inside the largest identified-ligand binding pocket: to mention E127, L124 and K379, which at least suggest an apparent mechanistic basis for inhibition of VMAT2. Besides, the simulated molecular dynamics confirmed the binding stability of tubocurarine at the docking site; eigenvalue analysis demonstrated highly adaptable protein-ligand complex, whereas covariance analysis showed functionally relevant residue correlations.

Concisely put, the elastic network analysis revealed a mixed kind of rigid and flexible contacts that proposed the possibility for tubucurarine to modulate VMAT2 function by means of some unique dynamic mechanism. These results taken together certainly place tubocurarine as a rather interesting candidate for drug development with VMAT2 as one of its targets, experimentally validating and optimizing selective actions while minimizing the off-target effects.

5. References

1. Shafie A, Ashour AA, Anwar S, Anjum F, Hassan MI. Exploring molecular mechanisms, therapeutic strategies, and clinical manifestations of Huntington's disease. Archives of Pharmacal Research. 2024 Jun;47(6):571-95. https://doi.org/10.1007/s12272-024-01499-w
2. Ast A, Roth L, Brusendorf L, Schindler F, Ammar OW, Berberich S, Edel J, Bonsor M, Georgii E, Hänig C, Langnick C. Formation of amyloid-like HTTex1 aggregates in neurons, downregulation of synaptic proteins and early mortality of Huntington's disease flies are causally linked. bioRxiv. 2025 Feb 7:2025-02. https://doi.org/10.1101/2025.02.06.636778
3. Gupta H, Perkins W, Stark C, Kikkeri S, Kakazu J, Kaye A, Kaye AD. Deutetrabenazine for the treatment of chorea associated with Huntington's disease. Health Psychology Research. 2022 Jun 28;10(5):36040. https://doi.org/10.52965/001c.36040
4. Akkol EK, Karatoprak GŞ, Carpar E, Hussain Y, Khan H, Aschner M. Effects of Natural Products on Neuromuscular Junction. Current Neuropharmacology. 2022

Mar 1;20(3):594-610. https://doi.org/10.2174/1570159X19666210924092627

5. Duarte JM, Dutta S, Goodsell DS, Burley SK. Exploring protein symmetry at the RCSB Protein Data Bank. Emerging topics in life sciences. 2022 Jul 8;6(3):231-43. https://doi.org/10.1042/ETLS20210267
6. Bittrich S, Segura J, Duarte JM, Burley SK, Rose Y. RCSB protein Data Bank: exploring protein 3D similarities via comprehensive structural alignments. Bioinformatics. 2024 Jun;40(6):btae370. https://doi.org/10.1093/bioinformatics/btae370
7. Altunkulah E, Ensari Y. Protein Structure Prediction: an in-Depth Comparison of Approaches and Tools. Eskişehir Teknik Üniversitesi Bilim ve Teknoloji Dergisi-C Yaşam Bilimleri Ve Biyoteknoloji. 2024;13(1):31-51. https://doi.org/10.18036/estubtdc.1378676
8. Ghosh D, Ghosh Dastidar D, Roy K, Ghosh A, Mukhopadhyay D, Sikdar N, Biswas NK, Chakrabarti G, Das A. Computational prediction of the molecular mechanism of statin group of drugs against SARS-CoV-2 pathogenesis. Scientific Reports. 2022 Apr 14;12(1):6241. https://doi.org/10.1038/s41598-022-09845-y
9. Almalki NA, Al-Abbasi FA, Moglad E, Afzal M, Al-Qahtani SD, Alzarea SI, Imam F, Sayyed N, Kazmi I. Protective activity of hirsutidin in high-fat intake and streptozotocin-induced diabetic rats: In silico and in vivo study. Heliyon. 2024 Oct 15;10(19). https://doi.org/10.1016/j.heliyon.2024.e38625
10. Ajayi II, Fatoki TH, Alonge AS, Balogun TC, Nwagwe OR, Moge GM, Shityakov S. In Silico ADME, Molecular Targets, Docking and Molecular Dynamics Simulation of Key Phytoconstituents of Lobelia inflata. Journal of Computational Biophysics and Chemistry. 2024 Dec 20;23(10):1359-73. https://doi.org/10.1142/S2737416524500480
11. Kim S, Chen J, Cheng T, Gindulyte A, He J, He S, Li Q, Shoemaker BA, Thiessen PA, Yu B, Zaslavsky L. PubChem 2023 update. Nucleic acids research. 2023 Jan 6;51(D1):D1373-80. https://doi.org/10.1093/nar/gkac956
12. Gan JH, Liu JX, Liu Y, Chen SW, Dai WT, Xiao ZX, Cao Y. DrugRep: an automatic virtual screening server for drug repurposing. Acta Pharmacologica Sinica. 2023 Apr;44(4):888-96. https://doi.org/10.1038/s41401-022-00996-2
13. Kulkarni VS, Alagarsamy V, Solomon VR, Jose PA, Murugesan S. Drug repurposing: an effective tool in modern drug discovery. Russian journal of bioorganic chemistry. 2023 Apr;49(2):157-66. https://doi.org/10.1134/S1068162023020139
14. Al-Shabib NA, Khan JM, Malik A, Rehman MT, Alamri A, Kumar V, Saris PE, Husain FM, AlAjmi MF. Multispectroscopic and computational insights into amyloid fibril formation of alpha lactalbumin induced by sodium hexametaphosphate. Scientific Reports. 2024 Dec 3;14(1):1-5. https://doi.org/10.1038/s41598-024-80897-y
15. Gan JH, Liu JX, Liu Y, Chen SW, Dai WT, Xiao ZX, Cao Y. DrugRep: an automatic virtual screening server for drug repurposing. Acta Pharmacologica Sinica. 2023 Apr;44(4):888-96. https://doi.org/10.1038/s41401-022-00996-2
16. Shahab M, Al-Madhagi H, Zheng G, Zeb A, Alasmari AF, Alharbi M, Alasmari F, Khan MQ, Khan M, Wadood A. Structure based

virtual screening and molecular simulation study of FDA-approved drugs to inhibit human HDAC6 and VISTA as dual cancer immunotherapy. Scientific Reports. 2023 Sep 2;13(1):14466. https://doi.org/10.1038/s41598-023-41325-9

17. Aziz M, Ejaz SA, Zargar S, Akhtar N, Aborode AT, A. Wani T, Batiha GE, Siddique F, Alqarni M, Akintola AA. Deep learning and structure-based virtual screening for drug discovery against NEK7: a novel target for the treatment of cancer. Molecules. 2022 Jun 25;27(13):4098. https://doi.org/10.3390/molecules27134098
18. Kondapuram SK, Sarvagalla S, Coumar MS. Docking-based virtual screening using PyRx Tool: autophagy target Vps34 as a case study. InMolecular docking for computer-aided drug design 2021 Jan 1 (pp. 463-477). Academic Press. https://doi.org/10.1016/B978-0-12-822312-3.00019-9
19. Khan MK, Ahmad S, Rabbani G, Shahab U, Khan MS. Target- based virtual screening, computational multiscoring docking and molecular dynamics simulation of small molecules as promising drug candidate affecting kinesin- like protein KIFC1. Cell Biochemistry and Function. 2022 Jul;40(5):451-72. https://doi.org/10.1002/cbf.3707
20. Ja'afaru SC, Uzairu A, Bayil I, Sallau MS, Ndukwe GI, Ibrahim MT, Moin AT, Mollah AM, Absar N. Unveiling potent inhibitors for schistosomiasis through ligand-based drug design, molecular docking, molecular dynamics simulations and pharmacokinetics predictions. Plos one. 2024 Jun 26;19(6):e0302390. https://doi.org/10.1371/journal.pone.0302390
21. Baroroh U, Biotek M, Muscifa ZS, Destiarani W, Rohmatullah FG, Yusuf M. Molecular interaction analysis and visualization of protein-ligand docking using Biovia Discovery Studio Visualizer. Indonesian Journal of Computational Biology (IJCB). 2023 Jul 21;2(1):22-30. https://doi.org/10.24198/ijcb.v2i1.46322
22. Khan MK, Ahmad S, Rabbani G, Shahab U, Khan MS. Target- based virtual screening, computational multiscoring docking and molecular dynamics simulation of small molecules as promising drug candidate affecting kinesin- like protein KIFC1. Cell Biochemistry and Function. 2022 Jul;40(5):451-72.https://doi.org/10.1002/cbf.3707
23. Di Biase C. Design, Synthesis and Biological Evaluation of Novel Dopamine D2/D3 Receptor Ligands (Doctoral dissertation, Dissertation, Düsseldorf, Heinrich-Heine-Universität, 2025).
24. Kakarala KK, Jamil K. Identification of novel allosteric binding sites and multi-targeted allosteric inhibitors of receptor and non-receptor tyrosine kinases using a computational approach. Journal of Biomolecular Structure and Dynamics. 2022 Aug 29;40(15):6889-909. https://doi.org/10.1080/07391102.2021.1891140
25. Nguyen TL, Samuel Leon Magdaleno J, Rajjak Shaikh A, Choowongkomon K, Li V, Lee Y, Kim H. Designing a multi-epitope candidate vaccine by employing immunoinformatics approaches to control African swine fever spread. Journal of Biomolecular Structure and Dynamics. 2023 Nov 24;41(19):10214-29. https://doi.org/10.1080/07391102.2022.2153922

26. Gaur NK, Ghosh B, Goyal VD, Kulkarni K, Makde RD. Evolutionary conservation of protein dynamics: Insights from all-atom molecular dynamics simulations of 'peptidase'domain of Spt16. Journal of Biomolecular Structure and Dynamics. 2023 Mar 4;41(4):1445-57. https://doi.org/10.1080/07391102.2021.2021990

27. Santra D, Maiti S. Molecular dynamic simulation suggests stronger interaction of Omicron-spike with ACE2 than wild but weaker than Delta SARS-CoV-2 can be blocked by engineered S1-RBD fraction. Structural Chemistry. 2022 Oct;33(5):1755-69. https://doi.org/10.1007/s11224-022-02022-x

HOW TO CITE THIS ARTICLE

Komal Kasegaonkar*, Shonak Adivarekar , Tejaswini Biraje , Babaso Udugade: Tubocurarine as a novel vmat2 inhibitor for huntington's disease: computational discovery, binding mechanism, and molecular dynamics insights. International Journal of Institutional Pharmacy and Life Sciences, Vol 15[2] March-April 2025 : 51-67.